

REPORT DOCUMENTATION PAGE				Form Approved OMB No. 0704-0188	
The public reporting burden for this collection of information is estimated to average 1 hour per response, including the time for reviewing instructions, searching existing data sources, gathering and maintaining the data needed, and completing and reviewing the collection of information. Send comments regarding this burden estimate or any other aspect of this collection of information, including suggestions for reducing this burden, to Department of Defense, Washington Headquarters Services, Directorate for Information Operations and Reports (0704-0188), 1215 Jefferson Davis Highway, Suite 1204, Arlington, VA 22202-4302. Respondents should be aware that notwithstanding any other provision of law, no person shall be subject to any penalty for failing to comply with a collection of information if it does not display a currently valid OPM control number. PLEASE DO NOT RETURN YOUR FORM TO THE ABOVE ADDRESS.					
1. REPORT DATE (DD-MM-YYYY) 18-06-2014		2. REPORT TYPE Technical Report		3. DATES COVERED (From - To)	
4. TITLE AND SUBTITLE Determination of an Optimal Control Strategy for a Generic Surface Vehicle				5a. CONTRACT NUMBER	
				5b. GRANT NUMBER	
				5c. PROGRAM ELEMENT NUMBER	
				5d. PROJECT NUMBER	
6. AUTHOR(S) Thomas A. Wettergren David B. Segala David Chelidze				5e. TASK NUMBER	
				5f. WORK UNIT NUMBER	
				8. PERFORMING ORGANIZATION REPORT NUMBER	
				TR 12,158	
7. PERFORMING ORGANIZATION NAME(S) AND ADDRESS(ES) Naval Undersea Warfare Center Division 1176 Howell Street Newport, RI 02841-1708				10. SPONSORING/MONITOR'S ACRONYM NUWC	
9. SPONSORING/MONITORING AGENCY NAME(S) AND ADDRESS(ES) Naval Undersea Warfare Center Division 1176 Howell Street Newport, RI 02841-1708				11. SPONSORING/MONITORING REPORT NUMBER	
12. DISTRIBUTION/AVAILABILITY STATEMENT Approved for public release; distribution is unlimited.					
13. SUPPLEMENTARY NOTES					
14. ABSTRACT Optimal path planning and control of vehicles becomes of greater importance as more and more tasks are transferred to autonomous agents. The concept of optimal path planning and optimal control of a generic surface vehicle in a constant current flow was investigated. This report documents the development of a three degree-of-freedom model of a generic surface vehicle and describes optimal path planning in a uniform surface current flow environment. The nominal path is derived using a two-point boundary value problem solution with constant propulsion. Optimal control strategy to follow the identified motion path starting from a randomly perturbed initial condition was also investigated and tested using the developed model. It was shown that in a relatively uniform surface current flow environment, the direct path from the initial point to the target location is optimal in terms of expended energy, where the least expended energy corresponds to constant thrust motion with the relative vehicle heading perpendicular to the flow.					
15. SUBJECT TERMS Autonomous Vehicles Boundary Value Problem Dynamic Programming Surface Vehicles Optimal Control Path Planning					
16. SECURITY CLASSIFICATION OF:			17. LIMITATION OF ABSTRACT SAR	18. NUMBER OF PAGES 30	19a. NAME OF RESPONSIBLE PERSON Thomas A. Wettergren
a. REPORT Unclassified	b. ABSTRACT Unclassified	c. THIS PAGE Unclassified			19b. TELEPHONE NUMBER (Include area code) 401-832-1559

20141024076

Determination of an Optimal Control Strategy for a Generic Surface Vehicle

Thomas A. Wettergren
David B. Segala
NUWC Division Newport

David Chelidze
University of Rhode Island



**Naval Undersea Warfare Center Division
Newport, Rhode Island**

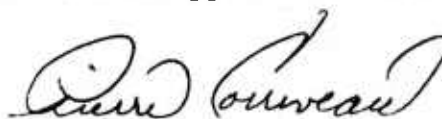
Approved for public release; distribution is unlimited.

PREFACE

This report was prepared under the Naval Undersea Warfare Center Division Newport Summer Faculty Program for summer 2013.

The technical reviewer for this report was John G. Baylog (Code 2511).

Reviewed and Approved: 18 June 2014



**Pierre J. Corriveau
Chief Technology Officer**



TABLE OF CONTENTS

	Page
INTRODUCTION	1
PLANAR SURFACE VEHICLE MODEL	2
NUMERICAL BENCHMARKING OF MODEL	5
TWO-POINT BOUNDARY VALUE PROBLEM AND CONTINUATION	9
NOMINAL PATH PLANNING FOR SURFACE VEHICLES.....	10
OPTIMAL CONTROL TO FOLLOW THE NOMINAL PATH.....	13
TESTING THE OPTIMAL CONTROL PROCEDURE.....	16
LIMITING CONTROL INPUT MAGNITUDE IN OPTIMAL CONTROL.....	19
SUMMARY AND CONCLUSIONS	23
REFERENCES	24

LIST OF ILLUSTRATIONS

Figure	Page
1 Schematic of a Generic Surface Vehicle	2
2 Sample Motion Trajectories Generated by the Vehicle for $V_x^f = 0.02$ m/s and $V_y^f = 0.01$ m/s	5
3 Sample Motion Trajectories Generated by the Vehicle for $V_x^f = 0.02$ m/s and $V_y^f = 0.01$ m/s	6
4 Sample Motion Trajectories Generated by the Vehicle for No Applied Thrust, $V_x^f = 0.02$ m/s and $V_y^f = 0.01$ m/s, and $v = 1.7$ m/s Initial Relative Velocity and $r = 10$ rad/s Angular Velocity.....	7
5 Sample Motion Trajectories Generated by the Vehicle for No Thrust But with $v = 1.7$ m/s Initial Relative Velocity and $r = 10$ rad/s Angular Velocity, $V_x^f = 0.2$ m/s and $V_y^f = 0.2$ m/s.....	8
6 Geometry for Vehicle NP Planning	10
7 Energy Required to Reach the Goal Versus Ratio of Time Spent Free-Floating over Time Spent on Powered Motion	12

LIST OF ILLUSTRATIONS (Cont'd)

Figure	Page
8 Various Achievable Trajectories with Constant Thrust Propulsion (Left Plot) and the Corresponding Energy Scaling with the Divergence from the Straight-Line Path (Right Plot)	12
9 NP Used in Control Testing.....	16
10 Optimal Control Applied to the Perturbed Initial Condition	17
11 Adjustments to the Applied Thrust Needed for Optimal Control in Figure 10	18
12 Blow-Up Near the Initial Time of the Optimal Control Shown in Figure 10.....	18
13 Difference Between the Nominal and Actual Trajectories for the Optimal Control Given in Figure 10.....	18
14 Optimal Constrained Control Applied to the Perturbed Initial Condition.....	19
15 Optimal Constrained Control Applied to the Perturbed Initial Condition.....	20
16 Applied Thrust Variations Needed for Control Shown in Figure 15.....	20
17 Difference Between the Nominal and Actual Trajectories for the Optimal Control Given in Figure 15.....	21
18 Optimal Constrained Control Applied to the Perturbed Initial Condition.....	22
19 Applied Thrust Variations Needed for Control Shown in Figure 18.....	22
20 Difference Between the Nominal and Actual Trajectories for the Optimal Control Given in Figure 18.....	22

DETERMINATION OF AN OPTIMAL CONTROL STRATEGY FOR A GENERIC SURFACE VEHICLE

INTRODUCTION

A critical component of all autonomous mechanical systems is the ability to follow prescribed motion trajectories. In particular, for autonomous vehicles, this motion trajectory is given by the determination of the motion path for the vehicle to follow to get from one point to another. Determining the best path to take and performing the mechanical functions to follow that path (that is, setting a thrust and steering) are basic functions of all driving and piloting that are often taken for granted when the vehicle is a manned (or remotely operated) system. For autonomous military systems, however, optimal path planning and optimal vehicle control are not simple, routine functions; they are complex operations affected by many parameters. As more and more tasks are transferred to autonomous agents, determining an optimal control strategy becomes increasingly crucial to system performance to assure platform safety, platform efficiency, and successful mission completion.

This report documents the research that was conducted to determine an optimal control strategy for a generic surface vehicle. Specifically, this report focuses on planning the optimal path for a generic surface vehicle (boat) that is operating in a region with non-negligible surface currents. Given a known initial position, the planning goal for this investigation was to find a path to get to a prescribed ending position at a prescribed time, while expending a minimal amount of energy. The steps necessary to achieve that goal, described in the ensuing sections, include such topics as (1) a mathematical description of a dynamic model of the surface vehicle, (2) a numerical investigation showing the qualitative validity of the model, (3) a two-point boundary value problem formulation of the path planning goal, (4) the optimization performed to determine those optimal paths, (5) techniques of optimal control theory to achieve the optimal path, even in situations when the initial condition is varied, (6) use of optimal control methods to provide a path that is close to the optimal trajectory, even when the available thrust for the vehicle is limited.

In short, this report demonstrates a method for determining the optimal trajectory and then using optimal control to best follow that trajectory in practical situations. All of the results presented in this report are simulation results run in MATLAB on a generic model of surface vehicles operating in currents.

PLANAR SURFACE VEHICLE MODEL

This study used a generic three degree-of-freedom surface vehicle model (figure 1) that considers surge, sway, and yaw dynamics and neglects heave, roll, and pitch dynamics.¹ The vehicle-fixed coordinate system is positioned at the center of mass with linear translational velocities $\{u, v\}$ and rotational velocity $\{r = \dot{\theta}\}$. Similarly, the interial (earth-fixed) reference frame $\{X, Y\}$ is positioned at the center of mass of the vehicle with linear translational velocities $\{\dot{x}, \dot{y}\}$ and rotational velocity $\{\dot{\theta}\}$.

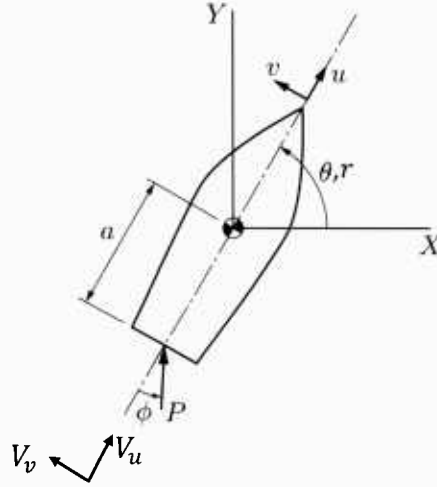


Figure 1. Schematic of a Generic Surface Vehicle

The rotation transformation matrix (equation (1)) used to map between vehicle-fixed and interial coordinates is given by:

$$\begin{bmatrix} \dot{x} \\ \dot{y} \\ \dot{\theta} \end{bmatrix} = \begin{bmatrix} \cos \theta & -\sin \theta & 0 \\ \sin \theta & \cos \theta & 0 \\ 0 & 0 & 1 \end{bmatrix} \begin{bmatrix} u \\ v \\ r \end{bmatrix}. \quad (1)$$

In the vehicle-fixed reference frame, the dynamics of the vehicle can be written as shown in equation (2):

$$M\dot{\eta} + C(\eta)\eta + D(\eta)\eta = f, \quad (2)$$

where $\eta = [u \ v \ r]^T$ is a state vector, M is the added mass and interial matrix, C is the Coriolis and centripetal matrix, D is the damping matrix, and f are the control forces and moments. The mass matrix M and Coriolis and centripetal matrix C can be further decomposed as shown in equation (3)

$$M = M_{RB} + M_A \text{ and } C = C_{RB} + C_A. \quad (3)$$

The mass matrix (equation (4)) is composed of rigid body contributions (that is, mass and inertia) and contributions from the surrounding fluid (that is, “added mass”). The mass matrix can be written as

$$M = \begin{bmatrix} m - X_{\dot{u}} & 0 & 0 \\ 0 & m - Y_{\dot{v}} & mx_g - Y_{\dot{r}} \\ 0 & mx_g - Y_{\dot{r}} & I_z - N_{\dot{r}} \end{bmatrix}, \quad (4)$$

where the following constants are used:

$$\begin{aligned} m &= 153.94 \text{ kg} \\ I_z &= 73.04 \text{ kg m}^2 \\ X_{\dot{u}} &= -18.17 \text{ kg} \\ Y_{\dot{v}} &= -124.54 \text{ kg} \\ Y_{\dot{r}} &= 0 \text{ kg m} \\ N_{\dot{r}} &= -36.15 \text{ kg m}. \end{aligned}$$

The Coriolis and centripetal matrix is written as shown in equation (5):

$$C(\eta) = \begin{bmatrix} 0 & 0 & m(x_g r + v) - (Y_{\dot{v}} v - Y_{\dot{r}} r) \\ 0 & Y_{\dot{v}} & m - X_{\dot{u}} u \\ -m(x_g r + v) + Y_{\dot{v}} v + Y_{\dot{r}} r & (-X_{\dot{u}} + m)u & 0 \end{bmatrix}. \quad (5)$$

The damping matrix is composed of linear and nonlinear terms. The linear damping is due to laminar friction on the body of the vehicle, and the nonlinear damping results from vortex shedding off the hull of the vehicle. The composite damping matrix is written as shown in equation (6):

$$D = D_L + D_{NL}(\eta) = \begin{bmatrix} X_u & 0 & 0 \\ 0 & Y_v & Y_r \\ 0 & N_v & N_r \end{bmatrix} + \begin{bmatrix} X_{u|u}|u| & 0 & 0 \\ 0 & Y_{v|v}|v| & 0 \\ 0 & 0 & N_{r|r}|r| \end{bmatrix}, \quad (6)$$

where the following constants are used:

$$\begin{aligned} X_u &= -107.33 \text{ kg/s} \\ Y_v &= -536.67 \text{ kg/s} \\ Y_r &= -322.00 \text{ kg m/s} \\ N_v &= -128.80 \text{ kg m/s} \\ N_r &= -1073.33 \text{ kg m}^2/\text{s} \\ X_{u|u} &= -107.33 \text{ kg/m} \end{aligned}$$

$$Y_{v|v|} = -536.67 \text{ kg/m}$$

$$N_{r|r|} = -322.00 \text{ kg m}^2.$$

The control force and moment vector is written as shown in equation (7):

$$f = \begin{bmatrix} P \cos \phi \\ P \sin \phi \\ a P \sin \phi \end{bmatrix}, \quad (7)$$

where a is the distance from the bow of the vehicle to the center of mass and P is the applied thrust at an angle ϕ .

Next, external forcing in the model was considered in the form of a constant current flow (V_x^f and V_y^f) in the vehicle-fixed reference frame. The implementation of these equations can be implemented into MATLAB and integrated using ODE45 (MATLABs ordinary differential equation solver). The equations can be rewritten in the inertial frame of reference as a set of six, first-order ODEs as follows (equation (8)) where $\tilde{(\cdot)}$ represents the relative difference between the velocity component and the current flow in that direction:

$$\begin{bmatrix} \dot{x} \\ \dot{u} \\ \dot{y} \\ \dot{v} \\ \dot{\theta} \\ \dot{r} \end{bmatrix} = N^{-1} \begin{bmatrix} \cos \theta & -\sin \theta & 0 \\ X_u + X_{u|u|}|\tilde{u}| & mr & -(Y_v \tilde{v} - Y_r r) \\ \sin \theta & \cos \theta & 0 \\ mr & Y_v + Y_{\tilde{v}} + Y_{v|v|}|\tilde{v}| & Y_r - X_{\tilde{u}} \tilde{u} \\ 0 & 0 & 1 \\ Y_{\tilde{v}} \tilde{v} + Y_r r & N_v - X_{\tilde{u}} \tilde{u} & N_r + N_{r|r|}|r| \end{bmatrix} \begin{bmatrix} \tilde{u} \\ \tilde{v} \\ r \end{bmatrix} + N^{-1} \begin{bmatrix} 0 \\ P_u \\ 0 \\ P_v \\ 0 \\ a P_v \end{bmatrix}, \quad (8)$$

where

$$N = \begin{bmatrix} 1 & 0 & 0 & 0 & 0 & 0 \\ 0 & m - X_{\tilde{u}} & 0 & 0 & 0 & 0 \\ 0 & 0 & 1 & 0 & 0 & 0 \\ 0 & 0 & 0 & m - Y_{\tilde{v}} & 0 & -Y_r \\ 0 & 0 & 0 & 0 & 1 & 0 \\ 0 & 0 & 0 & -Y_{\tilde{r}} & 0 & I_z - N_r \end{bmatrix}, \quad \begin{cases} \tilde{u} = u - V_u^f \\ \tilde{v} = v - V_v^f \end{cases}$$

$$V_u = V_x^f \cos \theta + V_y^f \sin \theta, \quad \text{and}$$

$$V_v = -V_x^f \sin \theta + V_y^f \cos \theta.$$

NUMERICAL BENCHMARKING OF MODEL

To test the model performance, the dynamic response due to several initial conditions was investigated; the resulting motion trajectories are shown in figures 2 through 5. In each case, the vehicle starts at $[0,0]$. For the case depicted in figure 2, the current flow in the horizontal and vertical dimensions are $V_x^f = 0.02$ m/s and $V_y^f = 0.01$ m/s, respectively. The vehicle is propelled by $P_u = P \cos \phi = 10$ N thrust in the u -direction, and $P_v = P \sin \phi = 50$ N thrust in the v -direction. A trajectory length of only 2 minutes is shown starting from a position aligned with the flow and zero-relative velocity with respect to the water. In figure 2, plot (A) shows the surface trajectory of the vehicle, plot (B) shows the vehicle displacements, plot (C) shows velocity, and plot (D) shows orientation and angular rate versus time. During the 2-minute trajectory, the vehicle rotated at a constant angular rate and translated in both X- and Y-directions. According to plot (B), the vehicle traversed a greater distance in the X-direction than in the Y-direction—a result of the applied thrust in the Y-direction, which produced a torque on the vehicle and caused the vehicle to rotate (plot D). Furthermore, the vehicle experienced a current flow that was twice as great in magnitude in the X-direction than in the Y-direction.

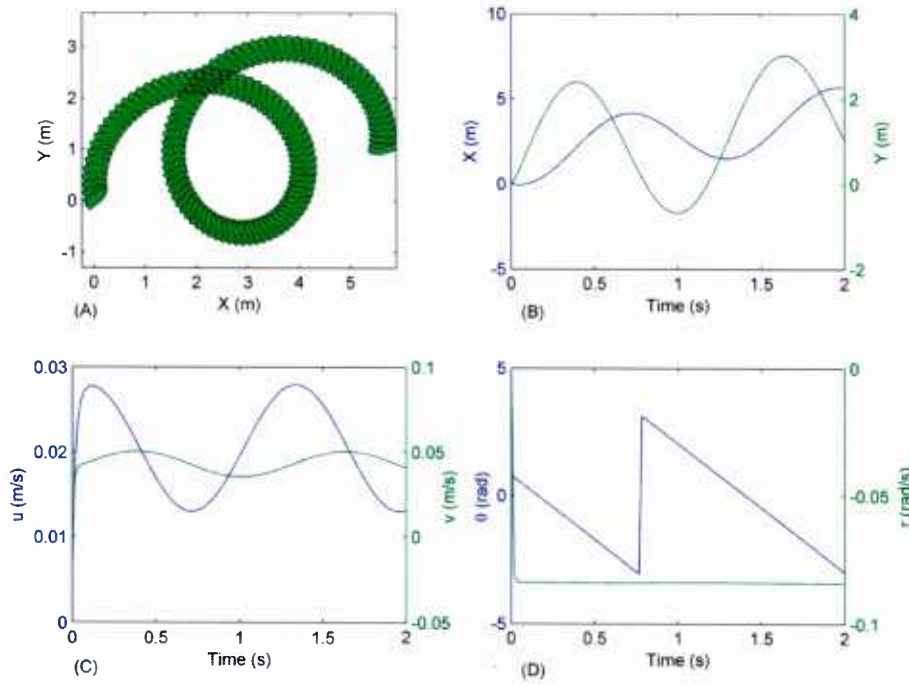


**Figure 2. Sample Motion Trajectories Generated by the Vehicle
for $V_x^f = 0.02$ m/s and $V_y^f = 0.01$ m/s**

(The vehicle is propelled by $P_u = 10$ N thrust in the u -direction and $P_v = 50$ N thrust in the v -direction. Plot (A) shows the surface trajectory of the vehicle, plot (B) shows the vehicle displacements, plot (C) shows velocity, and plot (D) shows orientation and angular rate versus time.)

Figure 3 depicts the response if the thrust is changed to $P_u = 1$ N and $P_v = 50$ N. The same dynamic behavior is seen in this sample trajectory as in the first case depicted in figure 2; however, with such a decrease of applied thrust in the X-direction, the vehicle rotated more in the same amount of time. The same type of response was observed in the first case (figure 2) except there were more rotations. Again, the vehicle rotated at a constant angular velocity.

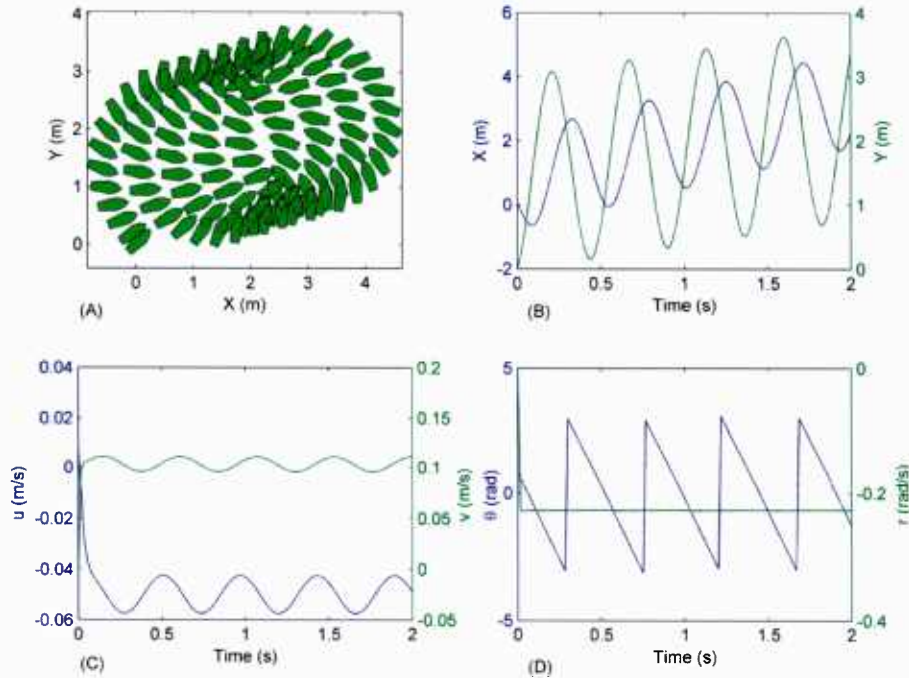


**Figure 3. Sample Motion Trajectories Generated by the Vehicle
for $V_x^f = 0.02$ m/s and $V_y^f = 0.01$ m/s**

(The vehicle is propelled by $P_u = 1$ N thrust in the u-direction and $P_v = 50$ N thrust in the v-direction. Plot (A) shows the surface trajectory of the vehicle, plot (B) shows the vehicle displacements, plot (C) shows velocity, and plot (D) shows orientation and angular rate versus time.)

Figure 4 depicts the effects if there is no applied thrust in either direction and an initial relative linear and angular velocity of $v = 1.7$ m/s and $r = 10$ rad/s, respectively. Without an applied thrust, the displacement increased linearly and the velocity, rotation, and angular velocity all remained constant after the transients decay due to the initial conditions. The steady-state response was reached within $t = 0.1$ s. The large jump in plot (A) between the first and second vehicle plot is a result of the initial condition. At the first time step, the vehicle is located at $[0,0]$ with the prescribed initial conditions. At the second time step, as a result of the dynamics, the velocity decreased to almost zero and rotation became constant; however, during this time step, a significant change in Y-displacement occurred.

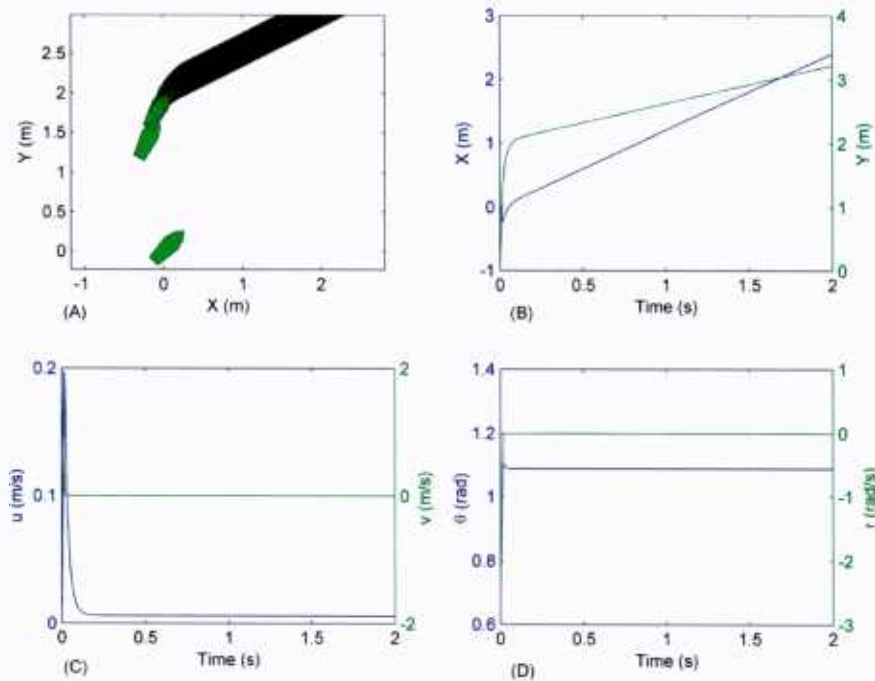


Figure 4. Sample Motion Trajectories Generated by the Vehicle for No Applied Thrust,
 $V_x^f = 0.02$ m/s and $V_y^f = 0.01$ m/s, and $v = 1.7$ m/s Initial Relative Velocity
and $r = 10$ rad/s Angular Velocity
(Plot (A) shows the surface trajectory of the vehicle, plot (B) shows the vehicle displacements,
plot (C) velocity, and plot (D) shows orientation and angular rate versus time.)

Figure 5 depicts the last numerical benchmark of the vehicle model. The same conditions were used as in the previous case (figure 4); however, the current flow was increased to $V_x^f = 0.2$ m/s and $V_y^f = 0.2$ m/s. Again, the same type of response was observed; the difference is the distance that was traveled in both the X- and Y-directions is a result of the increased current flow. Again, the large displacement observed in plot (A) is a result of the initial condition.

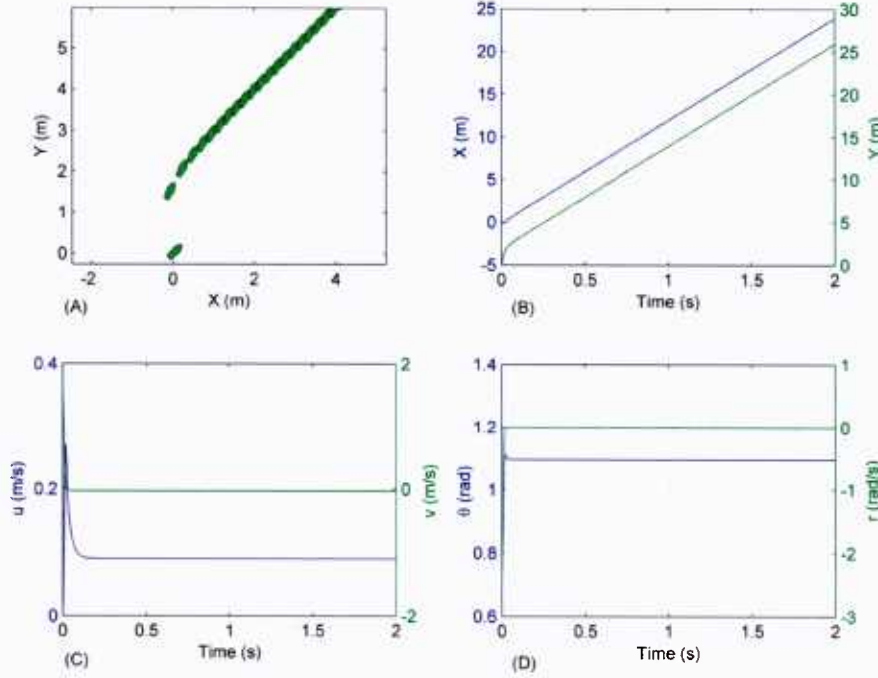


Figure 5. Sample Motion Trajectories Generated by the Vehicle for No Thrust but with $v = 1.7$ m/s Initial Relative Velocity and $r = 10$ rad/s Angular Velocity, $V_x^f = 0.2$ m/s and $V_y^f = 0.2$ m/s
(Plot (A) shows the surface trajectory of the vehicle, plot (B) shows the vehicle displacements, plot (C) shows velocity, and plot (D) shows orientation and angular rate versus time.)

TWO-POINT BOUNDARY VALUE PROBLEM AND CONTINUATION

The overall goal of this investigation is to determine a path for a generic surface vehicle to follow that passes between two waypoints in a predetermined fixed amount of time. Without loss of generality, only two waypoints will be considered. The proposed method is not concerned if these waypoints are the start and end locations of a specific mission, or if they are interior waypoints in a larger path-planning exercise. The overarching problem of determining a trajectory between two points with a given time can be expressed mathematically as a two-point boundary value problem (BVP). The standard practice lends itself to solving these problems using methods such as finite difference, shooting, and collocation.^{2,3} Other techniques to determine optimal paths involve heuristic procedures that are tuned to specific application contexts⁴ and are thus difficult to apply when a specific optimization objective is required. The two-point BVP described in the following paragraphs uses the numerical procedure in MATLAB's BVP (`bvp4c`) algorithm using the continuation method.

The goal is to find a solution to the set of first-order ODEs that were previously presented that model a generic surface vehicle on the time interval $[0, T]$ subject to two-point boundary value conditions:

$$\begin{aligned}
 x(0) - 0 &= 0 \\
 u(0) - V_u &= 0 \\
 y(0) - 0 &= 0 \\
 v(0) - V_v &= 0 \\
 r(0) - 0 &= 0 \\
 x(T) - X_T &= 0 \\
 y(T) - Y_T &= 0
 \end{aligned} \tag{9}$$

where the initial position is at zero-time from zero-position with zero-relative and angular velocities, and the final position is (X_T, Y_T) in time T . In addition to the motion trajectory, the solution to the BVP should also provide the initial orientation $\theta(0)$ and propulsion parameters (P_u, P_v) . Generally, there are multiple solutions to this particular BVP, but the MATLAB's `bvp4c` function will find the trajectory and thrust parameters based on an initial guess of the solution.

Solving the BVP problem using `bvp4c` requires an initial guess for the solution. Note that the algorithm is very sensitive to the particular form of the initial guess. The quality of the initial guess is paramount in convergence speed of the BVP algorithm and often determines if the solution can be determined practically. To facilitate finding a good initial guess that will converge to the solution, if available, one should use some *a priori* information about the system or the solution. If some intermediate solution is known, one can use continuation^{2,3} to solve the BVP sequentially by incrementing parameters from the known intermediate solution to the needed one—the method that was adopted in this work to find convergent solutions.

NOMINAL PATH PLANNING FOR SURFACE VEHICLES

Before determining an optimal path for the vehicle to follow to the desired end location or waypoint, a nominal path must first be determined. The nominal path (NP) is defined as *the path that requires minimal extended propulsion energy*. For this investigation, a constant, slow surface current in an arbitrary direction η was assumed. There is an intuitive supposition that sometimes it is beneficial (in terms of expended energy) to go against the flow for a short period of time and then just ride the current to the target without any propulsion. In particular, here we tested a hypothesis that, if the goal is achievable, then *the straight-line path to the target is the most economical*.

The schematic of a test configuration is shown in figure 6. The objective is to reach point $B (X_T, Y_T)$ in a fixed time T starting from point $O (0,0)$ while expending minimal energy. Two strategies for reaching the goal B were considered: (1) a straight-line motion to the goal (that is from O to B) and (2) first getting to the current flow streamline that passes through the goal (that is, from O to A) and then just riding that streamline to the goal (that is, from A to B) with no thrust. Note that the most efficient way to get to the streamline is to head perpendicular to it ($\theta = \pi/2 + \eta$).

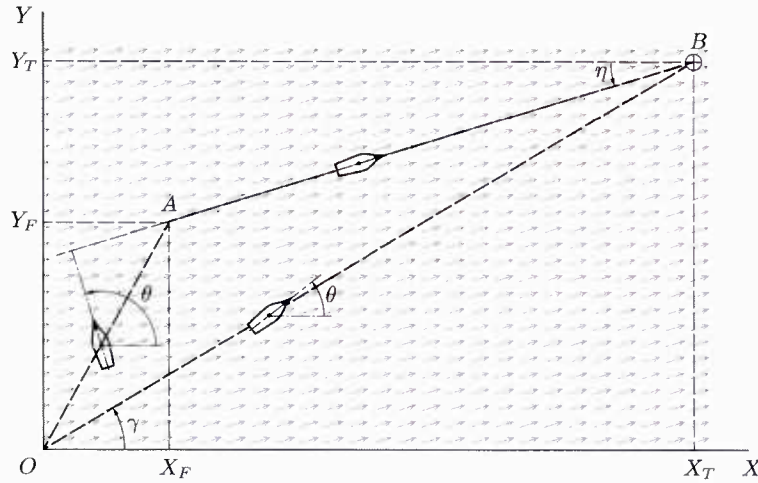


Figure 6. Geometry for Vehicle NP Planning

In practice, there would be some energy spent reorienting the vehicle at point A once the thrust is set to zero, but it is assumed that spent energy is small and negligible. Even if this energy is not negligible, it will only add to the cost of getting to the streamline. The most economical constant amplitude thrust for the powered straight-line motions from O to B , or O to A was used. Time spent going across the current is denoted T_C and time spent gliding along the current is denoted T_F , hence the overall travel time is $T = T_C + T_F$.

In the first scenario (strategy 1), $T = T_C$, then the average velocity required to reach the goal is $V^B = d_{B/O}/T$, where $d_{B/O}$ is a distance between points B and O . In addition, if the

corresponding average relative velocity of the vehicle with respect to the water is greater than the maximum possible vehicle velocity, the objective is unreachable. To calculate the actual thrust required for reaching the goal, the two-point BVP using the vehicle model (equation (8)) and the following initial and boundary conditions (equation (10)) were used:

$$\begin{bmatrix} x \\ u \\ y \\ v \\ \theta \\ r \end{bmatrix}_{t=0} = \begin{bmatrix} 0 \\ V_x^f \cos \theta + V_y^f \sin \theta \\ 0 \\ -V_x^f \sin \theta + V_y^f \cos \theta \\ \theta_0 \\ 0 \end{bmatrix}, \quad \begin{bmatrix} x \\ y \end{bmatrix}_{t=T} = \begin{bmatrix} X_T \\ Y_T \end{bmatrix}, \quad (10)$$

where $\theta_0 = \tan^{-1} \frac{V_y^B - V_y^f}{V_x^B - V_x^f}$. After determining the required constant thrust P , the total energy expended by the vehicle was determined by integrating the product of P_u with u (that is, the thrust and velocity in the u –direction, respectively) over the time of travel T (equation (11)):

$$E = \int_0^T P_u u dt \cong \sum_{k=1}^{N-1} P_k u_k \Delta t. \quad (11)$$

For the second scenario (strategy 2), the thrust required to get to point A was estimated using a continuation from the solution obtained for the straight-line motion scenario (first strategy). In this case, the average velocity during powered travel is $V^A = d_{A/O}/T_C$. In calculations, the time spent coasting along the current T_F was incremented from 0 to T_F^C , and the corresponding two-point (for the time from 0 to $T_C = T - T_F$) BVP was solved using the solution from the previous iteration step and the boundary conditions shown in equation (12):

$$\begin{bmatrix} x \\ u \\ y \\ v \\ \theta \\ r \end{bmatrix}_{t=0} = \begin{bmatrix} 0 \\ V_x^f \cos \theta + V_y^f \sin \theta \\ 0 \\ -V_x^f \sin \theta + V_y^f \cos \theta \\ \pi/2 + \eta \\ 0 \end{bmatrix}, \quad \begin{bmatrix} x \\ y \end{bmatrix}_{t=T_C} = \begin{bmatrix} X_F \\ Y_F \end{bmatrix}, \quad (12)$$

where T_F^C is a critical coasting time after which the objective is not reachable even using the maximum thrust available.

The results of the simulation are shown in figure 7, where the calculated expended energy is plotted versus the ratio of $\frac{T_F}{T_C}$. The resulting curve confirms the hypothesis that the most economical path to the goal is motion on a straight line when moving with constant thrust. A straight line, therefore, was chosen as an NP to the goal.

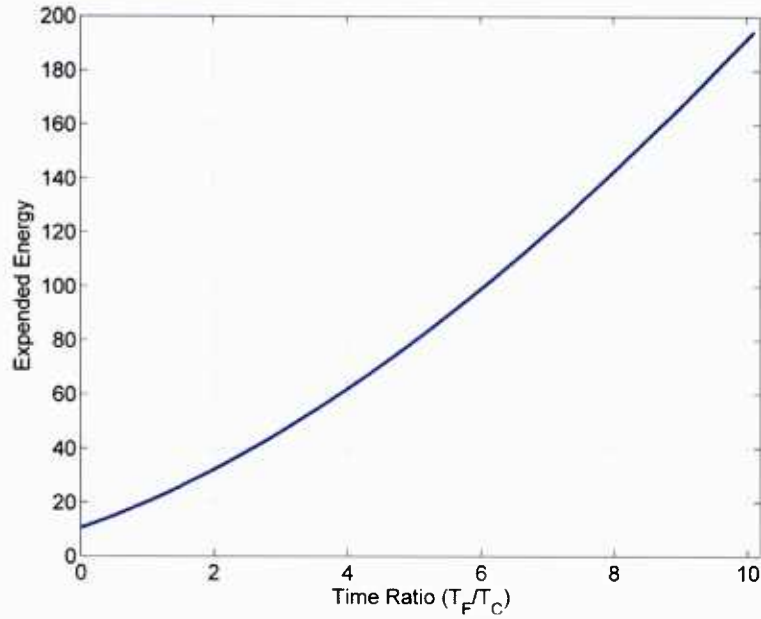


Figure 7. Energy Required to Reach the Goal Versus Ratio of Time Spent Free-Floating over Time Spent on Powered Motion

The formulation was modified to look at constant thrust motion from O to B with the different initial orientation of the vehicle mimicking the previous cases (strategies 1 and 2). In these cases there were no energy costs associated with the reorienting at point A . The BVP for each case was solved again using the results from the previous iteration while the angle was iterated from the initial required orientation for the straight-line motion to an additional 90° . The resultant motion trajectories are shown in the left plot in figure 8; the associated energy expended is shown in the right plot in figure 8.

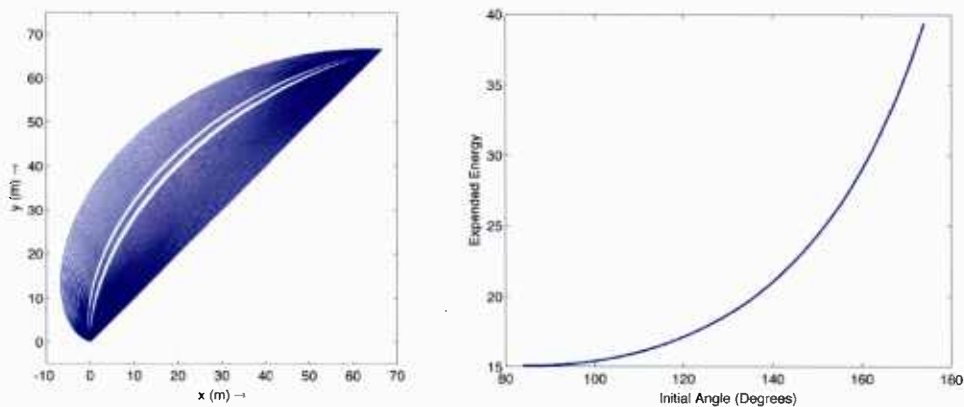


Figure 8. Various Achievable Trajectories with Constant Thrust Propulsion (Left Plot) and the Corresponding Energy Scaling with the Divergence from the Straight-Line Path (Right Plot)

OPTIMAL CONTROL TO FOLLOW THE NOMINAL PATH

It has been established that an NP for reaching a goal in fixed time is a straight-line path. For the NP, it was assumed that the vehicle's initial heading was parallel to the optimal heading and its initial relative velocity was zero. In practice, both assumptions are not realizable, and the vehicle could have any arbitrary initial heading and velocities within an allowable range. The vehicle equations have demonstrated that the vehicle is highly maneuverable (see figures 2 through 5) and can reorient itself within several seconds or minutes. Thus, the next step is to focus on developing an optimal control strategy^{5,6} that can be used to reorient the vehicle and follow the NP. During the simulations, it was observed that the controller's success was very sensitive to the size of the time step used in adjusting the control input. If the time step was kept small, the controller was stable; but if the time step was larger than the time it took to reorient the vehicle, the controller failed. In practice, one may want to split the control strategy into two stages: (1) initial reorientation (during which, the time step is kept small) followed by (2) NP tracking (for which, the time step can be increased substantially).

This investigation considered the vehicle model expressed in equation (13) for optimal control procedure:

$$\begin{bmatrix} \dot{x} \\ \dot{u} \\ \dot{y} \\ \dot{v} \\ \dot{\theta} \\ \dot{r} \end{bmatrix} = M^{-1} \begin{bmatrix} \cos \theta & -\sin \theta & 0 \\ X_u + X_{u|u}| \tilde{u} & mr & -(Y_v \tilde{v} - Y_r r) \\ \sin \theta & \cos \theta & 0 \\ mr & Y_v + Y_{\tilde{v}} + Y_{v|v}| \tilde{v} & Y_r - X_u \tilde{u} \\ 0 & 0 & 1 \\ Y_{\tilde{v}} \tilde{v} + Y_r r & N_v - X_u \tilde{u} & N_r + N_{r|r}|r| \end{bmatrix} \begin{bmatrix} \tilde{u} \\ \tilde{v} \\ r \end{bmatrix} + M^{-1} \begin{bmatrix} 0 \\ P_u \\ 0 \\ P_v \\ 0 \\ aP_v \end{bmatrix}, \quad (13)$$

where

$$M = \begin{bmatrix} 1 & 0 & 0 & 0 & 0 & 0 \\ 0 & m - X_{\dot{u}} & 0 & 0 & 0 & 0 \\ 0 & 0 & 1 & 0 & 0 & 0 \\ 0 & 0 & 0 & m - Y_{\dot{v}} & 0 & -Y_{\dot{r}} \\ 0 & 0 & 0 & 0 & 1 & 0 \\ 0 & 0 & 0 & -Y_{\dot{r}} & 0 & I_z - N_{\dot{r}} \end{bmatrix}, \quad \begin{cases} \tilde{u} = u - V_u^f \\ \tilde{v} = v - V_v^f \end{cases}$$

$$V_u = V_x^f \cos \theta + V_y^f \sin \theta, \quad \text{and}$$

$$V_v = -V_x^f \sin \theta + V_y^f \cos \theta.$$

Upon introduction of a state vector $z = [x, u, y, v, \theta, r]^T$, equation (13) is rewritten as:

$$\dot{z} = F(z, P).$$

The corresponding Jacobian matrices with respect to state and control variables are represented in equation (14):

$$\frac{\partial F}{\partial z} = M^{-1} \times \begin{bmatrix} 0 & \cos \theta & 0 & -\sin \theta & -u \sin \theta - v \cos \theta & 0 \\ 0 & X_u + 2X_{u|u}|\tilde{u}| & 0 & mr & r\Delta V_v + (X_u + 2X_{u|u}|\tilde{u}|)\Delta V_u & -(Y_{\tilde{v}}\tilde{v} - Y_{\tilde{r}}r) \\ 0 & \sin \theta & 0 & \cos \theta & u \cos \theta - v \sin \theta & 0 \\ 0 & mr & 0 & Y_v + Y_{\tilde{v}} + 2Y_{v|v}|\tilde{v}| & r\Delta V_u + (Y_v + Y_{\tilde{v}} + 2Y_{v|v}|\tilde{v}|)\Delta V_v & Y_r - X_{\tilde{u}}\tilde{u} \\ 0 & 0 & 0 & 0 & 0 & 1 \\ 0 & Y_{\tilde{v}}\tilde{v} + Y_{\tilde{r}}r & 0 & N_v - X_{\tilde{u}}\tilde{u} & \tilde{u}\Delta V_v + \tilde{v}\Delta V_u & N_r + 2N_{r|r}|r| \end{bmatrix}$$

$$\frac{\partial F}{\partial P} = M^{-1} \begin{bmatrix} 0 & 0 \\ 1 & 0 \\ 0 & 0 \\ 0 & 1 \\ 0 & 0 \\ 0 & a \end{bmatrix}, \quad (14)$$

where

$$\Delta V_u = V_x^f \sin \theta - V_y^f \cos \theta, \quad \text{and} \quad \Delta V_v = V_x^f \cos \theta + V_y^f \sin \theta.$$

Now, let t_k , which is uniformly distributed over time, be the times at which possible adjustments can be made to the control inputs. These time steps are separated by $h = \Delta t = T/N$. Let the current trajectory be z , denoting the NP \bar{z} , and the corresponding constant thrust \bar{P} . Then the deviation from the NP trajectory is defined as:

$$\Delta z(t_k) = z(t_k) - \bar{z}(t_k). \quad (15)$$

This deviation leads to the following linear discrete approximation to the equations of motion about the NP trajectory (equation (16)):

$$z_{k+1} = z_k + h \left. \frac{\partial F}{\partial z} \right|_{z=\bar{z}_k} \Delta z_k + h \frac{\partial F}{\partial P} (\bar{P} + \Delta P_k), \quad (16)$$

where $t_k = kh$, $z_k = z(t_k)$. Equation (16) is rewritten in equation (17):

$$z_{k+1} = A_k z_k + B_k (\bar{P} + \Delta P_k), \quad (17)$$

where

$$A_k = I + h \left. \frac{\partial F}{\partial z} \right|_{z=\bar{z}_k}, \quad \text{and} \quad B_k = h \frac{\partial F}{\partial P}.$$

An optimal control strategy for the vehicle was found based on equations (18), (19), and (20) by using dynamic programming. The optimal control goal was to minimize the following objective function:

$$\Gamma = \alpha z_N^T H z_N + (1 - \alpha) \sum_{k=1}^{N-1} z_k^T Q_k z_k + \Delta P_k^T R_k \Delta P_k \quad (18)$$

Using standard dynamic programming procedures,⁵ the gain used for control was calculated recursively for k from 1 to $N - 1$ using:

$$G_{N-k} = -[(1 - \alpha)R_{N-k} + B_{N-k}^T U_{k-1} B_{N-k}]^{-1} B_{N-k}^T U_{k-1} A_{N-k}, \quad (19)$$

where

$$U_k = V_{N-k}^T U_{k-1} V_{N-k} + (1 - \alpha) G_{N-k}^T R_{N-k} G_{N-k} + (1 - \alpha) Q_{N-k},$$

with

$$U_N = \alpha H, \quad \text{and} \quad V_{N-k} \triangleq A_{N-k} + B_{N-k} G_{k-1}.$$

The appropriate adjustment to the thrust at the k -th time step was then calculated as

$$\Delta P_k = G_k(z_k - \bar{z}_k). \quad (20)$$

The application of this thrust adjustment provided an optimal control that followed the stated trajectory as best as possible, given the constraints of the vehicle dynamics and available control authority.

TESTING THE OPTIMAL CONTROL PROCEDURE

The effectiveness of the optimal control procedure was demonstrated by testing it on a problem whose initial conditions were perturbations from the initial conditions used for determining the initial optimal path. The objective was to start in the vicinity of the (0,0) position and reach a target at $(X, Y) = (1000, 1000)$ m position in 50 minutes. We assume the current is 0.2 m/s in x -direction and -0.2 m/s in the y -direction. The NP was calculated by solving the corresponding BVP (see figure 9), where the nominal thrust was $P_u = 91.481$ N.

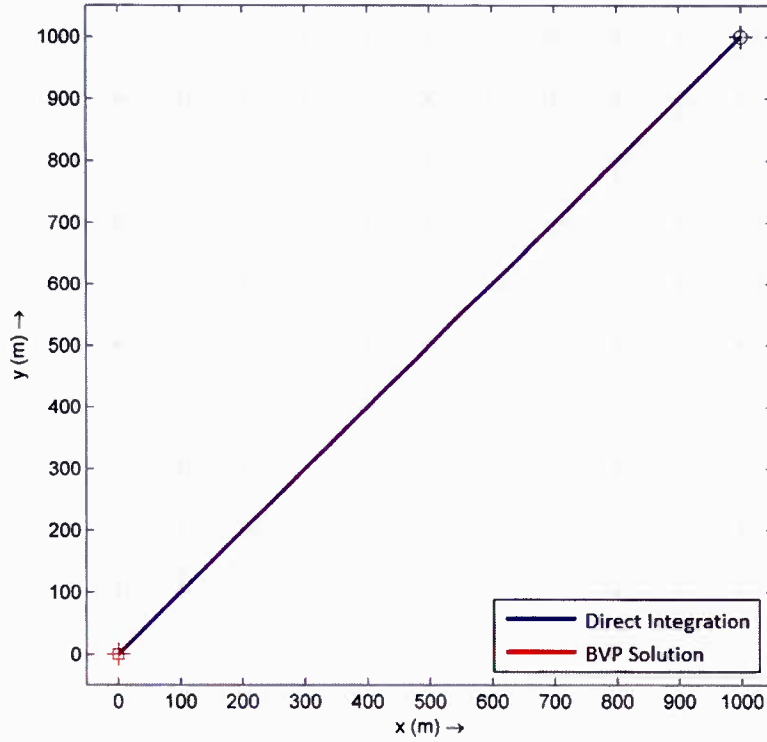


Figure 9. NP Used in Control Testing

The initial condition for NP $\overline{(\cdot)}$ (equation (21)) and the actual initial condition given to the control algorithm (equation (22)) are

$$\begin{bmatrix} \bar{x} \\ \bar{u} \\ \bar{y} \\ \bar{v} \\ \bar{\theta} \\ \bar{r} \end{bmatrix}_{t=0} = \begin{bmatrix} 0 \\ -0.1455 \\ 0 \\ -0.2425 \\ 1.3258 \\ 0 \end{bmatrix}, \quad (21)$$

$$\begin{bmatrix} x \\ u \\ y \\ v \\ \theta \\ r \end{bmatrix}_{t=0} = \begin{bmatrix} -1.3008 \\ 0.8824 \\ 10.7352 \\ 8.0658 \\ -2.7238 \\ 0 \end{bmatrix}. \quad (22)$$

For the objective function, we set $\alpha = 0.9$, and use the following matrices:

$$Q_k = \begin{bmatrix} 1 & 0 & 0 & 0 & 0 & 0 \\ 0 & 1 & 0 & 0 & 0 & 0 \\ 0 & 0 & 1 & 0 & 0 & 0 \\ 0 & 0 & 0 & 1 & 0 & 0 \\ 0 & 0 & 0 & 0 & 0 & 0 \\ 0 & 0 & 0 & 0 & 0 & 0 \end{bmatrix}, \quad H_k = \begin{bmatrix} 1 & 0 & 0 & 0 & 0 & 0 \\ 0 & 0 & 0 & 0 & 0 & 0 \\ 0 & 0 & 1 & 0 & 0 & 0 \\ 0 & 0 & 0 & 0 & 0 & 0 \\ 0 & 0 & 0 & 0 & 0 & 0 \\ 0 & 0 & 0 & 0 & 0 & 1 \end{bmatrix}, \quad \text{and} \quad R_k = \begin{bmatrix} 1 & 0 \\ 0 & 1 \end{bmatrix}. \quad (23)$$

The resulting trajectories are shown in figure 10; figure 11 shows the adjustments needed in the control inputs. Figure 12 shows a blowup of the resulting trajectories near the beginning of motion, and figure 13 shows the difference between the nominal and actual trajectories.

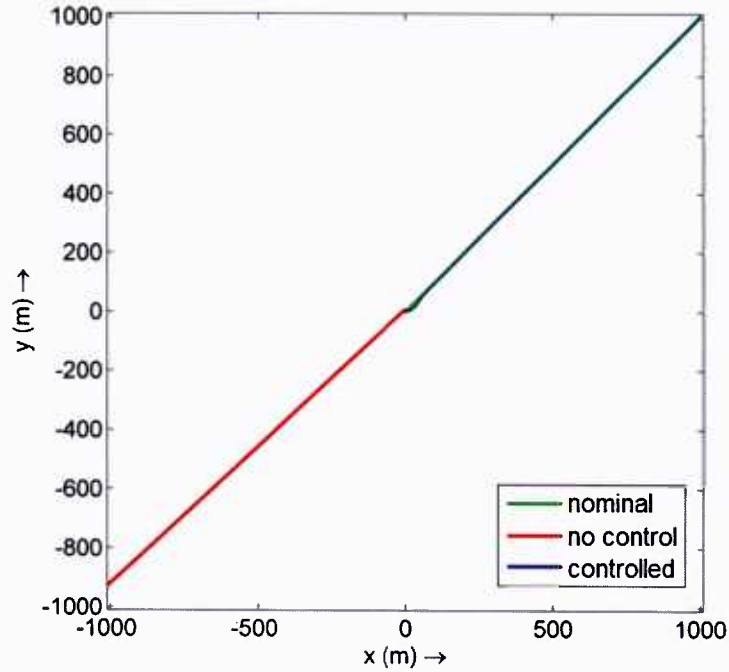


Figure 10. Optimal Control Applied to the Perturbed Initial Condition

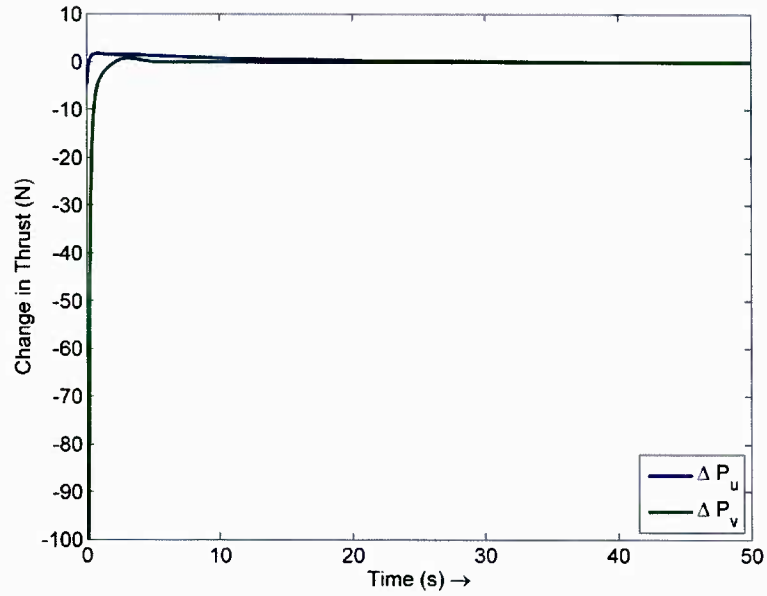


Figure 11. *Adjustments to the Applied Thrust Needed for Optimal Control in Figure 10*

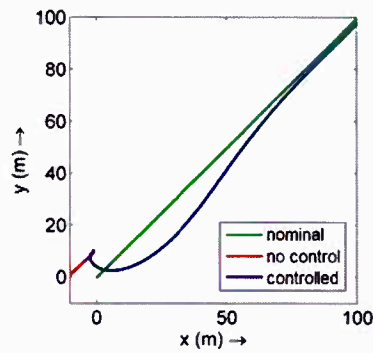


Figure 12. *Blow-Up Near the Initial Time of the Optimal Control Shown in Figure 10*

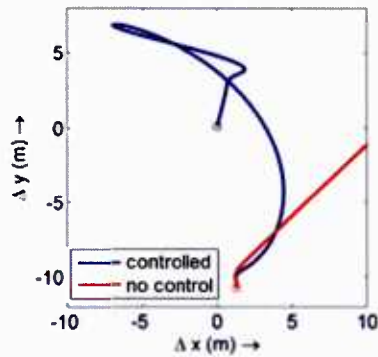


Figure 13. *Difference Between the Nominal and Actual Trajectories for the Optimal Control Given in Figure 10*

LIMITING CONTROL INPUT MAGNITUDE IN OPTIMAL CONTROL

In a more realistic environment, an unlimited amount of thrust is usually not available; therefore, any restrictions that meet a physical behavior or desired response can be incorporated into the optimal trajectory determination methodology. Generally, this problem is solved by incorporating a penalty function in the objective function or implementing a constrained optimal control procedure (using interior point methods). For this research, the clipping procedure was used; that is, the control inputs are clipped to a maximum amplitude. This control strategy was tested for several initial conditions; no significant degradation in controller performance was observed. The goal NP is shown in figure 14, where the objective needs to be reached in 10 seconds. The constant thrust estimated by solving the BVP for the NP was 91.628 N, and the maximum possible amplitude was set to be 125 N (as with all that follow).

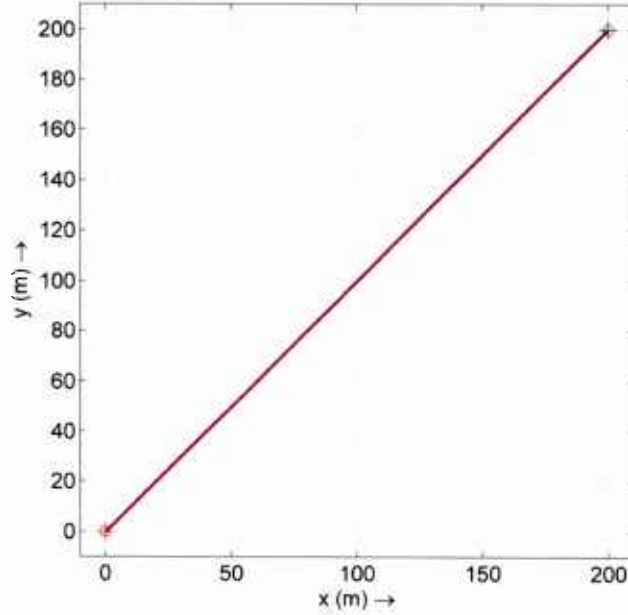


Figure 14. Optimal Constrained Control Applied to the Perturbed Initial Condition

Figure 15 shows the constrained controlled tracking of the NP; the corresponding clipped control inputs are shown in figure 16. The deviations between the nominal and actual trajectories are given in figure 17. The initial condition for the NP (equation (24)) and the actual initial condition given to the control algorithm (equation (25)) are

$$\begin{bmatrix} \bar{x} \\ \bar{u} \\ \bar{y} \\ \bar{v} \\ \bar{\theta} \\ \bar{r} \end{bmatrix}_{t=0} = \begin{bmatrix} 0 \\ -0.1455 \\ 0 \\ -0.2425 \\ 1.3258 \\ 0 \end{bmatrix}, \quad (24)$$

$$\begin{bmatrix} x \\ u \\ y \\ v \\ \theta \\ r \end{bmatrix}_{t=0} = \begin{bmatrix} -0.7860 \\ -5.3962 \\ -0.8570 \\ -2.7366 \\ -1.6118 \\ 0 \end{bmatrix}. \quad (25)$$

For the objective function, we set $\alpha = 0.95$, and all other matrices were the same.

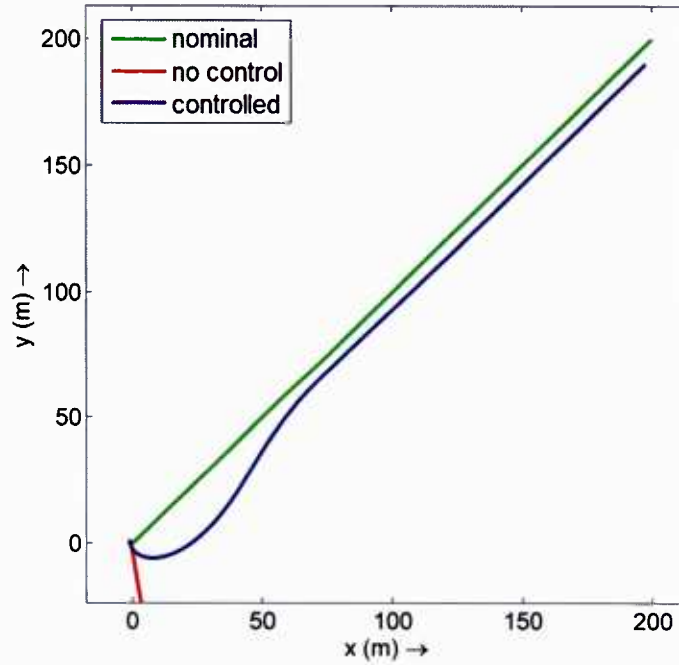


Figure 15. Optimal Constrained Control Applied to the Perturbed Initial Condition

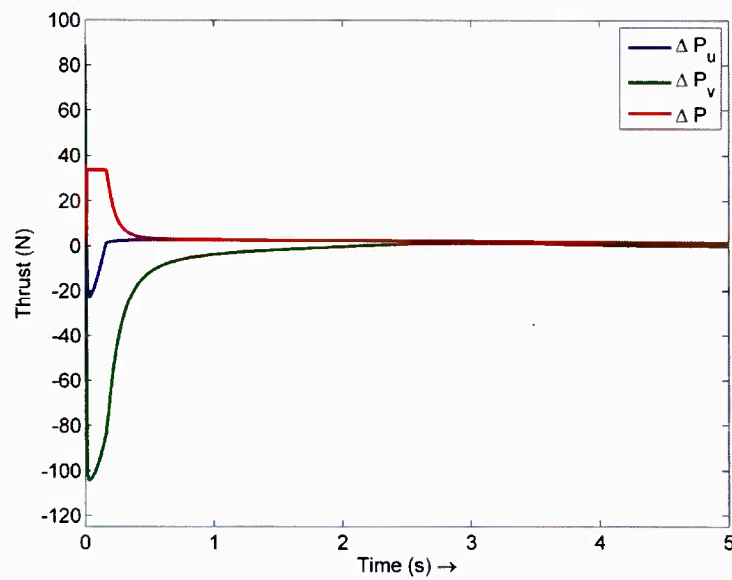


Figure 16. Applied Thrust Variations Needed for Control Shown in Figure 15

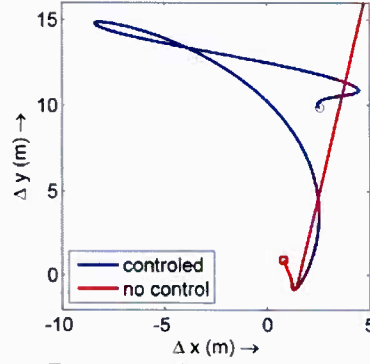


Figure 17. Difference Between the Nominal and Actual Trajectories for the Optimal Control Given in Figure 15

Figure 15 shows that it is clear that 10 s is not enough time to achieve the objective in this situation; therefore, simulations for a larger time and space for the exact same objective and NP shown in figure 9 were run. The results are shown in figures 18, 19, and 20 for when the initial condition for NP (equation (26)) and the actual initial conditions given to the control algorithm (equation (27)) are

$$\begin{bmatrix} \bar{x} \\ \bar{u} \\ \bar{y} \\ \bar{v} \\ \bar{\theta} \\ \bar{r} \end{bmatrix}_{t=0} = \begin{bmatrix} 0 \\ -0.1455 \\ 0 \\ -0.2425 \\ 1.3258 \\ 0 \end{bmatrix}, \quad (26)$$

$$\begin{bmatrix} x \\ u \\ y \\ v \\ \theta \\ r \end{bmatrix}_{t=0} = \begin{bmatrix} -3.4692 \\ -1.7462 \\ -6.0079 \\ 2.6502 \\ 2.8860 \\ 0 \end{bmatrix}. \quad (27)$$

It is clear from these extended-time trajectories that the allowance of additional time creates a more gradual deviation using moderate levels of thrust over the extended time. Also, the additional time allows for a controlled trajectory that does reach the goal point.

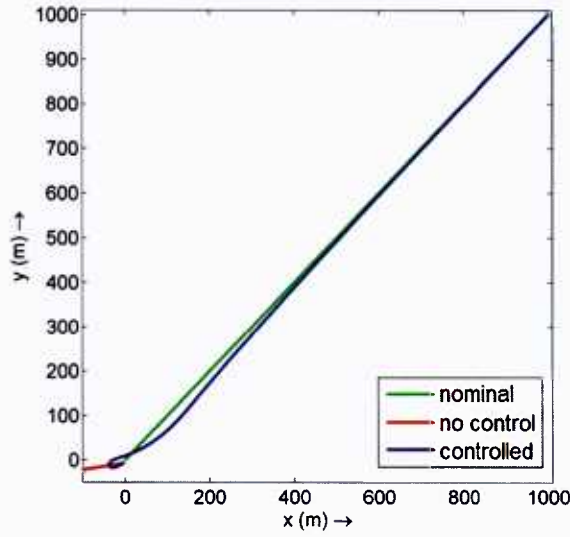


Figure 18. Optimal Constrained Control Applied to the Perturbed Initial Condition

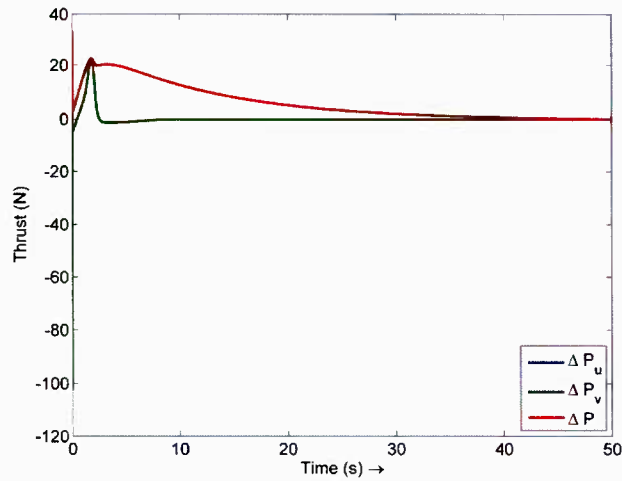


Figure 19. Applied Thrust Variations Needed for Control Shown in Figure 18

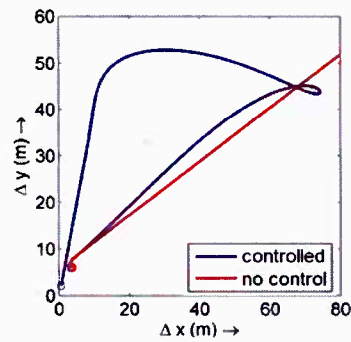


Figure 20. Difference Between the Nominal and Actual Trajectories for the Optimal Control Given in Figure 18

SUMMARY AND CONCLUSIONS

The concept of optimal path planning and optimal control of a generic surface vehicle in a constant current flow was investigated. A three degree-of-freedom, rigid-body model for a surface vehicle was developed, its parameters were estimated, and its performance was tested in simulations. The resulting model was used to estimate a nominal path of motion for a vehicle by solving a two-point boundary value problem. It was shown in a relatively static current flow that a straight-line constant thrust motion was optimal in terms of energy consumption. An optimal control algorithm was developed to follow the determined nominal path of motion and was extensively tested in various conditions. For sufficiently small time steps, the optimal control strategy was able to follow the nominal trajectory even when substantial perturbations were introduced in the initial conditions. The algorithm was also modified to limit range-of-control input values and was still capable of following pre-planned trajectory.

In more dynamic or nonlinear current flows, the solution of a two-point boundary value problem becomes more problematic and straight-line paths are no longer optimal. It is still feasible that the constant thrust motion will be the most advantageous even in these dynamic, nonlinear conditions. It may be possible to solve the two-point boundary value problem in a static nonlinear current flow environment, but some other path planning methodology is required for a dynamic flow/obstacle environment. Metaheuristic search methods to find the energy-efficient paths is one such possibility and is, in fact, the planned methodology for the next phase of this research.

REFERENCES

1. Thor I. Fossen, *Guidance and Control of Ocean Vehicles*, John Wiley and Sons, Ltd., Chichester, United Kingdom, 1994.
2. Uri M. Ascher, Robert M. M. Mattheij, and Robert D. Russell, *Numerical Solution of Boundary Value Problems for Ordinary Differential Equations*, Society for Industrial and Applied Mathematics, Philadelphia, 1995.
3. Forman S. Acton, *Numerical Methods that Work*, Mathematical Association of America, Washington, DC, 1990.
4. Steven M. LaValle, *Planning Algorithms*, Cambridge University Press, New York, 2006.
5. Donald E. Kirk, *Optimal Control Theory: An Introduction*, Prentice-Hall, Inc., Englewood Cliffs, NJ, 1970.
6. Robert F. Stengel, *Optimal Control and Estimation*, Dover Publications, Inc., New York, 1994.

INITIAL DISTRIBUTION LIST

Addressee	No. of Copies
University of Rhode Island (Mechanical Engineering - David Chelidze)	5
Defense Technical Information Center	2
Center for Naval Analyses	1